APPLICATION OF JUPYTER NOTEBOOK IN CROSS PLOTTING OF ROCK PROPERTIES DATASETS FOR LITHOLOGY AND FLUID DISCRIMINATION IN A NIGER DELTA OIL RESERVOIR, SOUTH-SOUTH NIGERIA

Supported by tetfund TERTIARY EDUCATION TRUST FUND

M. O. Ikponmwen[1], K. Itiowe[2], B. U. Iyemifokhae[1]
[1]Department of Physics, University of Benin, Benin-city, Edo State, Nigeria
[2]Department of Earth Sciences, Arthur Jarvis University, Akpabuyo, Cross River State, Nigeria
Corresponding author's email: kiamukeitiowe@yahoo.com
Received: March 20, 2022 **Accepted:** June 18, 2022

Abstract: Python language was used on Jupyter note book to cross plot rock properties for lithology and fluid discrimination by engaging well datasets from a given Niger Delta oil field. The data used for the analysis consist of suites of one well which included gamma ray logs, velocity log, resistivity and caliper log and some derived logs. Sand lithology showed low gamma ray, high resistivity and low acoustic impedance. After the cross plotting was carried out, the plots with the most outstanding results were λρ Versus Vp/Vs, μρ against Density and λρ versus μρ. For the oil well considered, one reservoir was observed at a depth of 2774 meters to 2835 meters (9100 ft. to 9300 ft.). Crossplotting of rock properties discriminated the lithology into sand and shale, which is typical of Niger Delta Region in South-South Nigeria. The crossplot also discriminated the fluids into gas, brine and oil. This study has been able to show that an open source program (Python) which is easily available and accessible online, can be engaged in carrying out hydrocarbon reservoirs characterization study, in lieu of the proprietary software that are popularly used in the industries but often difficult to access by academic researchers.
Keywords: Jupyter notebook, Crossplot, Hydrocarbon, Reservoirs Characterization.

Introduction

Lithology and pore fluid discrimination are important aspects of reservoir characterization which is a key input in any petroleum exploration and evaluation projects. Lithology and pore fluid discrimination finds applications in geologic studies, formation evaluation, reservoir modeling, well planning, enhancement of oil recovery processes, drilling as well as oil-well completion. Lithology generally refers to as the rock type in the earth. Different types of rocks occur in the subsurface of the earth, but not all are favorable for hydrocarbon accumulation. For a rock to sufficiently hold hydrocarbon, the rock should be sedimentary in nature, with pore spaces that are interconnected and while all elements of the hydrocarbon play elements must be in place. Knowledge derived from the rock type of a well can be used to deduce a range of parameters including pore fluid content (Agbasi *et al*. 2018).

Precise determination and understanding of lithology, pore fluid, pore sizes and shapes are elemental to Petrophysical studies. Accurate discrimination of lithology and pore fluid are some of the challenges for hydrocarbon exploration and development (Kupecz *et al*., 1997). The precise determination of lithology and pore fluid helps in the accurate determination of permeability, porosity and saturation. The productivity of a hydrocarbon field is depended on the quality and accurate determination of its lithology and pore fluid (Hami-Eddine et al.,2015).

Lithology and pore fluid can be explicitly determined using core samples derived from subsurface formation. Core sample analyses for lithology and pore fluid determination are exorbitant and usually time consuming to obtain good information (Chang *et al*., 2002). Cuttings obtained from drilling operations can provide information on the lithology and pore fluid. The flaw of using cuttings to determine lithology and pore fluid is that the recovery depths of the cuttings are usually undetermined (Akinyokun et al., 2009; Serra and Abbott, 1982). The use of well log data for determining lithology and pore fluid has been growing tremendously because it is more reliable and cheaper. Well logging provides the advantage of covering the entire area of interest and offers details of the subsurface formation (Serra and Abbott, 1982, Brigaud *et al*., 1990)

Rock Physics describes a reservoir rock by physical properties such as porosity, rigidity, compressibility; properties that will affect how seismic waves physically travel through the rocks. It establishes a relationship between elastic properties such as bulk and shear modulus, Vp/Vs; reservoir properties such as permeability, porosity, lithology, and architecture properties such as fractures (Saberi, 2013). In determining lithology, gamma ray log are used to differentiate sand from shale and calculating the volume of shale (Fens, 2000, Kurah *et al*., 2021).

Cross plots are visual presentations of the connection between two or more variables, and they are used to vividly detect or identify anomalies which could be interpreted as the presence of rock types and hydrocarbon or other fluids (Agbasi et al. 2018). Cross plot analysis are done to determine the rock attributes that better discriminate the reservoir properties (Omudu *et al*. 2007). AVO crossplotting typically used the intercept and gradient. Goodway *et al.* (1997) used crossplots of elastic parameters (Lambda-Rho and Mu-Rho) to improve petrophysical discrimination of rock properties.

The study area is located in the coastal swamp depositional belt (depobelt) within the Niger Delta oil province, as shown in the red oval (Fig. 1)

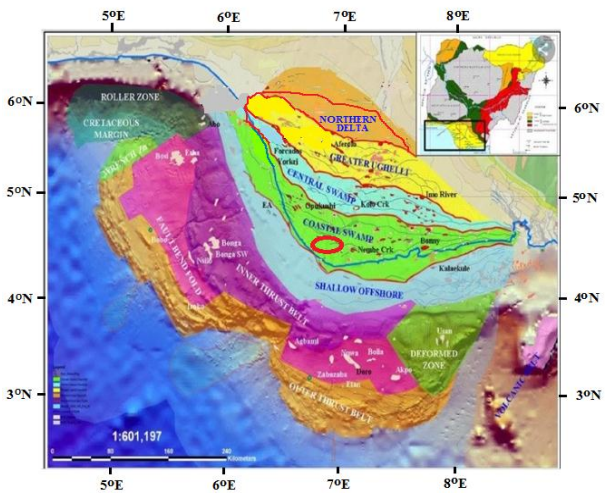

Figure 1. Location map of study area, indicated with the red spot (Oluwajana et al. 2017 and Tuttle et al. 1999).

Geologic setting

The Niger Delta Basin is situated at the Gulf of Guinea, which is part of the eastern Atlantic Ocean and spreads all through the Niger Delta province between longitude latitude 4ºN to 6ºN and 5ºE to 8ºE (Tuttle *et al.* 1999) (Fig. 2). The Niger Delta Basin consists of three geologic Formations namely: the marine Akata, paralic Agbada and continental Benin Formations (Frankl and Cordy, 1967; Avbovbo, 1978; Reijers, 2011; Itiowe *et al*., 2020) (Table 1). The Akata Formation is the primary source rock, and is made up of marine shale (Doust and Omatsola 1990). The reservoir rock of the Agbada Formation is made up of sandstone with shale intercalation (Itiowe and Lucas 2020a; Kiamuke *et al*., 2021), while the Benin Formation is made up of continental sand (Itiowe and Lucas, 2020b). According to Kulke (1995), during the formation of the delta, there was equilibrium between the rate of subsidence and sedimentation. The depositional pattern of the sediment was influenced by the tectonic setting and structural configuration of the terrain. The delta has prograded south-westwards from the Eocene to Recent forming five depositional belts at each stage of the formation (Doust and Omatsola 1990).

Table 1: Age and Formations of the Niger Delta Sedimentary Basin (modified after Short and Stauble 1969).

Subsurface			**Surface outcrop**		
youngest known age	**FORMATION**	**OLDEST KNOWN AGE**	**YOUNGEST KNOWN AGE**	**FORMATION**	**OLDEST KNOWN AGE**
Recent	Benin Fm.	Oligocene	Holocene	Alluvium	Miocene?
			Ear. Holo. To Late Pleistoc.	Deltaic Plain Deposits	
	Afam Shale Member		Plio. / Pleist.	Benin Fm.	
Recent	Agbada Fm.	Eocene	Miocene	Ogwashi - Asaba Fm.	Oligocene
			Eocene	Ameki Fm.	Eocene
Recent	Akata Fm.	Eocene	L. Eocene	Imo Shale	Paleocene
	Equivalent not known	Paleocene	Paleocene	Nsukka Fm.	Maestrich.
		Maestrich.	Maestrich.	Ajali Fm.	Maestrich.
			Campanian	Mamu Fm.	Campanian
			Camp./ Mae.	Nkporo Sh.	Santonian
			Conia/ Santo.	Agwu Shale	Turonian
			Turonian	Ezeaku Shale	Turonian
			Albian	Asu River Gp.	Albian

Data set and methodology

The dataset used for this study include basic logs such as caliper, gamma ray, resistivity and other derived logs such P wave velocity, S wave velocity Acoustic impedance (I_P), Shear Impedance (I_S). The well was analyzed in terms of lithology and fluid. Shale lithology was delineated by the high gamma ray value. Shale lithology causes the deflection of gamma ray log to the far right due to its radioactive nature, while we see higher density values around the non-reservoir areas as shown in Figure 2. Python language was used on Jupyter Notebook to plot all the log curves. Jupyter notebook a web-based interactive computational environment for creating Jupyter notebook documents. Its contains an ordered list of input/output cells which can contain code, text (using Markdown), mathematics, plots and rich media, usually ending with the ipython extension.

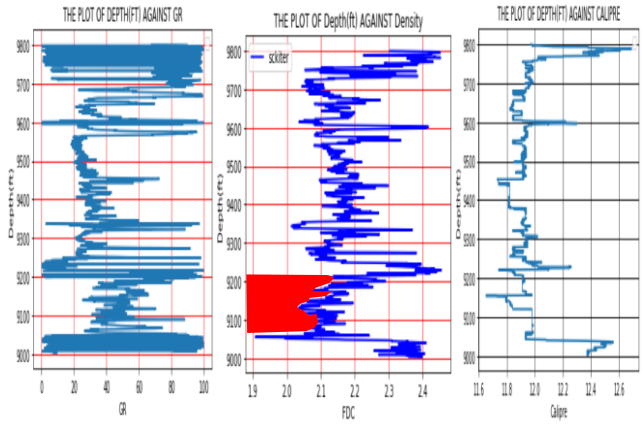

Figure 2: Logs used in the analysis: Gamma Ray, Density, Resistivity (After Goodway et al., 1997)

Theoretical Background

Biot-gassmann theory of velocity in porous rocks

The basic equations for P and S-wave velocity in isotropic, non-porous media are well known and can be written as:

$$V_p = \sqrt{\frac{\lambda+2\mu}{\rho}} = \sqrt{\frac{K+\frac{4}{3}\mu}{\rho}} \quad 1$$

$$V_s = \sqrt{\frac{\mu}{\rho}}$$

Where ρ is the density, λ is the 1st Lamé parameter, μ is the 2nd Lamé parameter or shear modulus, and K is the bulk modulus, or the inverse of compressibility. Since the P-wave velocity in equation (1) has been written in two separate ways, it is obvious that the relationship between K and λ, which can be written as equation (1) will be given by equation (2).

$$K\text{-}\lambda = \frac{2}{3}\mu \quad 2$$

This problem was first addressed by Biot (1941), and then Gassmann (1951) using apparently different approaches but, as shown by Krief *et al.* (1990), these two approaches lead to the same results. Although there have been many theories proposed since Biot and Gassmann, their method has remained the most robust and frequently implemented way of expressing the P- and S-wave velocities of porous rocks in terms of elastic constants.

Poisson's ratio

Poisson's ratio can be derived in several ways such as velocity method or Lambda- Mu-Rho (LMR) LMR method. In this work Poisson's ratio log was achieved by using velocity method calculation shown in equation (3).

$$\sigma_{dry} = \frac{\left[\frac{V_p}{V_s}\right]^2_{dry} - 2}{2\left[\frac{V_p}{V_s}\right]^2_{dry} - 2} \quad 3$$

W

Vp = P wave velocity

Vs = S wave velocity

Extracting the fluid term

Since we intend to apply this method to seismic data in a later study, a practical limitation that will be discussed later is that we can estimate only the P and S-wave impedances, Z_p and Z_s, rather than velocities V_p and V_s, where:

$$Z_s = \rho V_s = \sqrt{\rho\mu} \quad 4$$

$$Z_p = \rho V_p = \sqrt{\rho(f+s)} \quad 5$$

Lambda rho estimation

Goodway *et al*. (1997) have championed the use of the parameters $\lambda\rho$, $\mu\rho$, and λ/μ obtained from pre-stack seismic data. Here λ and μ are the elastic Lame´ parameters and ρ is the density. The Lame´ parameter μ is the same as the shear modulus. Goodway *et al*. (1997) use the approximation to the P–P reflectivity in terms of P- and S-wave impedances:

$$R_{pp}(\theta) = \frac{\Delta I_p}{2I_p}(1+\tan^2\theta) - 8\left(\frac{V_s}{V_p}\right)^2 \sin^2\theta \frac{\Delta I_s}{2I_s} - \left[\frac{1}{2}\tan^2\theta - 2\left(\frac{V_s}{V_p}\right)^2 \sin^2\theta\right]\frac{\Delta\rho}{\rho} \quad 6$$

Where Δ indicates contrast across the reflecting interface, and I_P, I_S, and ρ are the average P-wave impedance, the average S-wave impedance, and the average density over the interface. The average P-wave and S-wave velocities are denoted by V_p and V_s, and they are related to impedances in the usual way: $I_p = \rho V_p$, and $I_s = \rho V_s$. Ignoring the far-angle third term in density contrast, equation(6) can be used to extract P and S reflectivity sections from pre-stack P-wave data, which are then inverted to obtain I_P.

$$\lambda\rho = \sqrt{((Ip)^2 - 2(Is)^2)} \quad 7$$

Where:

$\lambda\rho$ = Lambda Rho

Vp = P wave velocity

Vs = S wave velocity

Ip = P wave impedance (Acoustic impedance)

I_s = S impedance

Results and discussion

This section shows results from crossplots of the various reservoir parameters and datasets engaged in this study. The cross plots analyses are useful in differentiating between fluid and lithology in the reservoir (Omudu *et al*. 2007). Cross plotting is widely used in AVO analysis, because it facilitates the simultaneous and meaningful evaluation of two attributes. Here we cross plotted appropriate pairs of attributes, so that common lithology and fluid types generally cluster together allows for straightforward interpretation.

Crossplot of Velocity Ratio vs. Poisson ratio (σ):

It is possible to identify hydrocarbon zones by investigating the relationship of Poisson's and $\frac{V_p}{V_s}$ ratio.

The Poisson's ratio log is shown in below (Figure 3 and 4). The hydrocarbon (gas zone) is represented by a rectangular part (Figure 4). We observe that the gas saturated formation possess very low Poisson's ratio compared to the surrounding formations in the well. For different lithologies of the same fluid, normally the shale lithology will plot at relatively higher Poisson's ratio than the sand lithology as seen in both the depth plot and Poisson's and $\frac{V_p}{V_s}$ ratio done in the python environment.

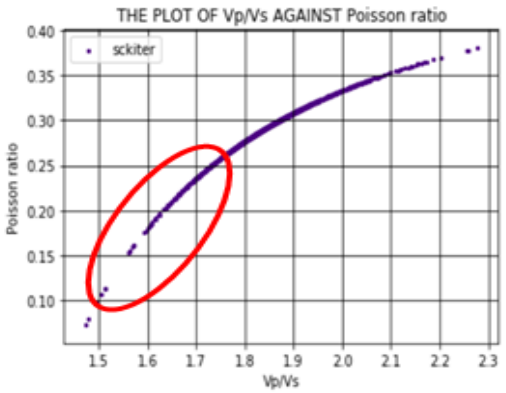

Figure 3: Poisson`s ratio versus $\frac{V_p}{V_s}$ crossplot. The gas sand reservoir captured by red ellipse

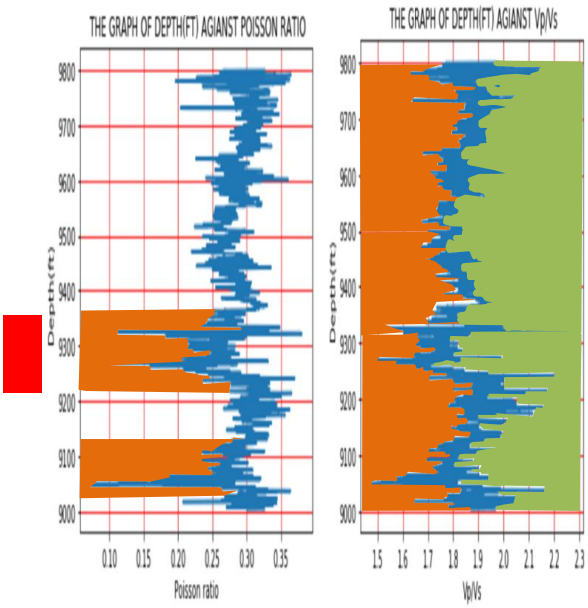

Figure 4: From left to right: Poisson's ratio and $\frac{V_p}{V_s}$ log for the well. The reservoir sand is characterized by low $\frac{V_p}{V_s}$ and Poisson's ratio values

Lambda-Rho (Incompressibility) against Mu-Rho:
Cross plots of Lambda Rho (λρ) against Mu Rho (μρ) shows separation into four zones that can be inferred to be probable shale(black eclipse), brine (yellow eclipse), oil (red eclipse) and gas zone (blue eclipse) confirmed by lowest density values (Figure 5). The plot indicates that λρ is more robust than μρ in the analysis of fluids in the field of study, and that μρ values are relatively low for the reservoir sand.This is also seen in the depth plot which has less peak values when compared with λρ within the reservoir region of 2774 meters to 2835 meters (9100 to 9300ft) (Figure 6).

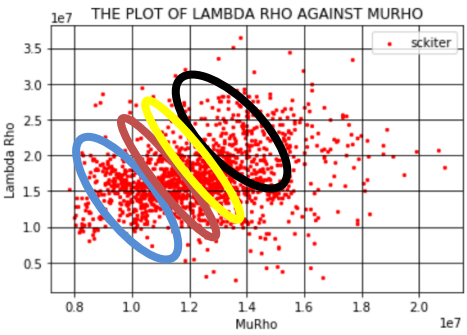

Figure 5: Crossplots of Lamda rho (λρ) against Mu rho (μρ)

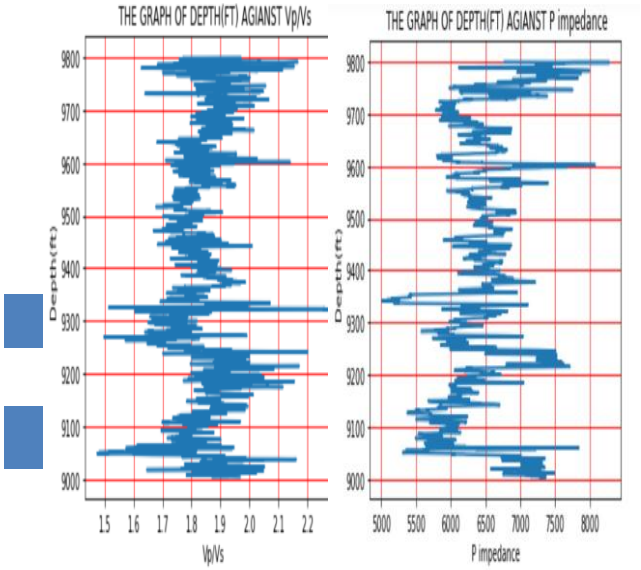

Figure 6: From left to right: Lambda Rho and Mu Rho variation with Depth (Well log)
V_p/V_s ratio against acoustic impedance

The crossplot of $\frac{V_p}{V_s}$ ratio against Acoustic impedance (Z_p) distinguishes the reservoir into two zones namely; hydrocarbon sand zone (orange ellipse) and shale zone (white ellipse) (Figure 7). Within the hydrocarbon sand we can also see a variation indicated by the red ellipse which may indicate possible gas sand. This crossplot shows better fluid as well as lithology discrimination along the acoustic impedance axis, indicating that acoustic impedance attribute will better describe the reservoir conditions in terms of lithology and fluid content than $\frac{V_p}{V_s}$ratio**.**Variation of Vp/Vs and P impedance (Acoustic impedance) down the well can be seen in figure 8.

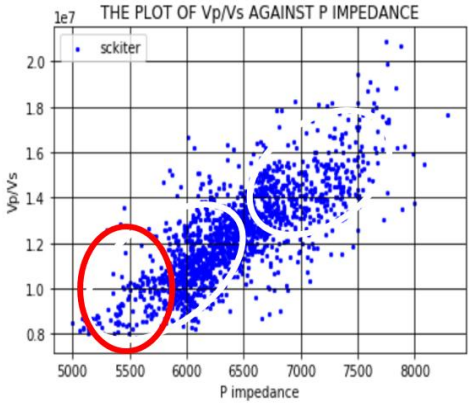

Figure 7: $\frac{V_p}{V_s}$ verse P impedance (Acoustic impedance) cross plot.

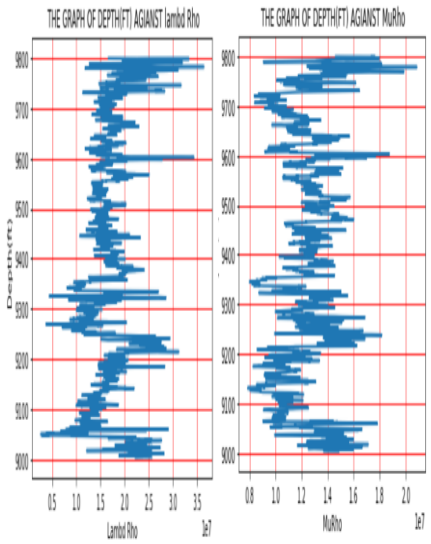

Figure 8: From left to right: Vp/Vs and P impedance (Acoustic impedance) log for the well

MU-RHO against Density

Both mu rho and density proved to be good lithology discriminators, with density also being a good fluid discriminator. Murho values are high for sand and low for shale (Figure 9). Conversely, the density of shale is higher than that of sand. Furthermore, brine is denser than hydrocarbon (oil and gas). Also as shown in the well records (Figure 10), a low density of about ~ 2.5 - 2 g/cc is observed in the sand reservoirs at 2804 meters to 2768 meters (9200ft – 9080ft) and also between 2949 meters to 2973 meters (9675ft – 9755ft), MuRho log which shows similar behavior. The density log is strongly affected by the presence of gas and record the lowest density values. The figure shows that there have been marked fall in the target area which suggest presence of hydrocarbon bearing sand, while the red section describes the shale region.

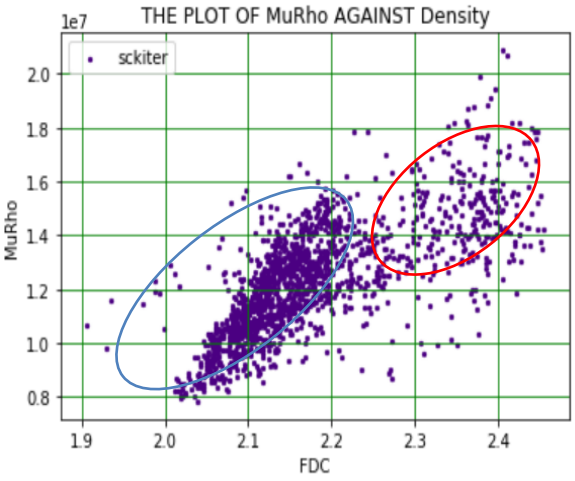

Figure 9: From left to right: MuRho and P Density log for the well

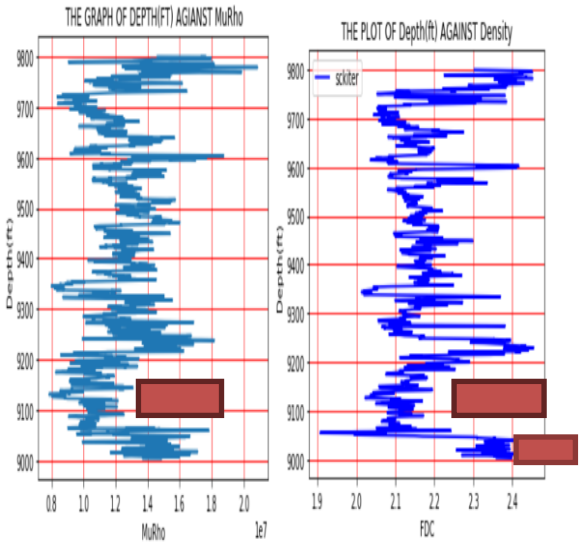

Fig 10: MuRho versus Density cross plot

Conclusion

The Acoustic impedance (Zp), Lambda-rho (λρ) and Mu-rho (μρ) attributes were found to be most robust in lithology and fluid discrimination within the reservoir in the cross plot analysis. The crossplots of P-impedance vs. Vp/Vs detect gas sands and shale.

The λ-μ-ρ technique was able to identify gas sands, because of the separation in responses of both the λρ and μρ sections to gas sands versus shale. Other lithologies could also be identified by the cross plot of λρ versus μρ. This is possible because each lithology has a different rock properties response that is subjected to fluid content and mineral properties.

References

Agbasi O. E., Chukwu G. U., Igboekwe M. U. and Etuk S. E. (2018). Pore Fluid and Lithology Discrimination of a Well in the Niger Delta Region using Elastic Parameters. World News of Natural Sciences. 17: 75-88.

Akinyokun O. C., Enikanselu P. A., Adeyemo A. B. and Adesida, A. (2009). Well log interpretation model for the determination of lithology and fluid contents. The Pacific Journal of Science and Technology 10, pp. 507-517.

Avbovbo A. A. (1978).Tertiary lithostratigraphy of Niger Delta: Amerian Association of Petroleum Geologists Bulletin, vol. 62, pp.295-300.

Biot M. A. (1941). General theory of Three-Dimensional consolidation. Journal of Applied Physics, 12, 155-164.

Brigaud F., Chapman D.S., Le Douaran S. (1990). Estimating thermal conductivity in Sedimentary Basin using lithological data and geophysical well logs.American Association of Petroleum Geologists Bulletin Vol. 74.No. 9. pp. 1459-1477

Chang H., Kopaska-Merkel D. C. and Chen H. (2002). Identification of lithofacies using Kohonen Self – Organizing Maps. Computers and Geosciences 28, pp. 223-229.

Doust H. E. and Omatsola E. M. (1990).Niger Delta. In: Edwards J. D. and Santagrossi, P. A (eds), Divergent/Passive Basins. AAPG. Bull. Mem. 45. Tulsa Okhlahoma pp. 201-238.

Fens T. W. (2000). Petrophysical properties from small rock samples using Image Analysis Technique.Pp.31, 32.Delft University Press, Stevinweg 1, 2628 CN, Delft, the Netherlands.

Frankl E. J. and Cordry E. A. (1967). The Niger Delta recent Developments Onshore and Offshore. 7th World Petroleum Congress, Mexico City, Proceedings, vol. 2, pp. 125-209.

Gassman F. (1951). Elastic waves through a packing sphere. Geophysics, 16: 673-685.

Goodway B., Chen Taiwen and Downton J. (1997). Improved AVO fluid detection and lithology discrimination using Lame petrophysical parameters; "λρ", "μρ", "λμ" fluid stack, from P and S inversions.

Hami-Eddine K., Klein P., Loic R., Ribet, B. and Grout M. (2015). A new technique for lithology and fluid content prediction from prestack data: An application to carbonate reservoir. Interpretation, 3(1), SC19-SC32.

Itiowe K. and Lucas F. A. (2020a). Palynological Zonation and Paleoclimatic Condition of the Sediments Penetrated by Ash-3 Well in the Greater Ughelli Depobelt, Niger Delta Basin. An International Journal of Pure and Applied Sciences, 19 (1), 37 – 48.

Itiowe K. and Lucas F. A. (2020b). Foraminiferal Biostratigraphy and Paleoenvironmental Study of the Sediments Penetrated within the interval of 6030ft. to 11115ft. of Ash-3 Well in the Greater Ughelli Depobelt, Niger Delta Basin. An International Journal of Pure and Applied Sciences, 19 (1),130 – 150.

Itiowe K., Lucas F. A. and Olise C. O. (2020). Foraminiferal Biostratigraphy and Paleoenvironmental analysis of the sediments penetrated by Sahaiawei-1 Well in the Northern Delta Depobelt, Niger Delta Basin. Global Journal of Geological Series, 18: 119-126.

Kiamuke I., Adebayo L. F. and Rorome O. (2021). Palynological and Paleoclimatic Conditions of the Sediments Penetrated by Sahaiawei-1 Well in the Northern Delta Depobelt, Niger Delta Basin. Journal of Mining and Geology. 5 (1), 47:54.

Kulke H. (1995). Nigeria, in, Kulke, H., ed., Regional Petroleum Geology of the World. Part II: Africa, America, Australia and Antarctica: Berlin, GebrüderBorntraeger, p. 143-172.

Kupecz J. A., Gluyas J. and Bloch S. (1997). Reservoir Quality Prediction in Sandstones and Carbonates: An Overview. American Association of Petroleum Geologists Volume 69. DOI: https://doi.org/10.1306/M69613

Kurah K. B., Shariatipour S. and Itiowe K. (2021). "Reservoir characterization and volumetric estimation of reservoir fluids using simulation and analytical methods: A case study of the coastal swamp depobelt, Niger Delta Basin, Nigeria". Journal of Petroleum Exploration and Production Technology (Springer Journal).11(6), 2347-2365.

Krief M., Garat J., Stellingwerff J. and Ventre J. (1990). A petrophysical interpretation using the velocities of P and S waves (Full-Waveform Sonic), The log analyst 31(06).

Oluwajana O. A., Ehinola O. A., Okeugo C. G. and Adegoke O. (2017). Modeling Hydrocarbon Generation Potentials of Eocene Source Rocks in the Agbada Formation, Northern Delta Depobelt, Niger Delta Basin, Nigeria'. Journal of Petroleum Exploration and Production Technology, 7, 379–388.

Omudu M. L. and J. O. Ebeniro S. Olotu. (2007), Optimizing Quantitative Interpretation for Reservoir Characterization: Case Study Onshore Niger Delta: A paper presented at the 31st Annual SPE International Technical Conference and Exhibition in Abuja, Nigeria.

Reijers T. J. A. (2011). Stratigraphy and Sedimentology of the Niger Delta. Geologos, vol. 17, no. 3, pp. 133-822.

Saberi M. R. (2013). Rock physics integration: From petrophysics to simulation. 10th Biennal International Conference and Expositions. P 444.

Serra O. and Abbott H. T. (1982). Contribution of logging data to sedimentology and stratigraphy. Society of Petroleum Engineers Journals 22 (01):117-131.

Short K. C. and Stauble A. J. (1967). Outline Geology of Niger Delta: AAPG Bulletin, vol. 51, pp.761-779.

Tuttle W. L. M., Brownfield E. M. and Charpentier R. R. (1999). The Niger Delta Petroleum System. Chapter A: Tertiary Niger Delta (Akata-Agbada) Petroleum System, Niger Delta Province, Nigeria, Cameroon and Equatorial Guinea, Africa. U.S. Geolgical Survey, Open File Report. 99-50-H.